Enhancement of the mode purity of shear horizontal mode of a thickness-shear transducer through design changes

Marco Zennaro and Dan J O'Boy
Department of Aeronautical and Automotive, Loughborough University
Loughborough, Leicestershire, LE11 3TU, United Kingdom
+44(0)1509227268
D.J.Oboy@lboro.ac.uk

P Mudge
TWI,
Granta Park, Cambridge, CB21 6AL, United Kingdom

Abstract
In ultrasonic guided waves, arrays of thickness-shear piezoelectric transducers are often used to generate Lamb and shear-horizontal waves in plates and longitudinal/torsional waves in pipes. The shear-horizontal modes (torsional modes in pipes) are particularly useful for guided wave testing. Although the ultrasonic output of such transducers are well known both numerically and experimentally, few results are available in the literature regarding the influence of geometry, electrode layout and materials on the ultrasonic output of the transducer: in particular, the influence of those parameters on the mode purity of the generated shear horizontal mode in plates requires further investigation. Numerical simulations with finite element modelling (Comsol Multiphysics) have been conducted on a thickness-shear transducer on a plate to understand the influence of these parameters. The study has been conducted both in frequency domain and time domain: the former was used to calculate the frequency response function of the transducer-waveguide system while the latter was used to verify the proportionality between different modes. Different configurations of the transducers have been designed and tested numerically, and the in- and out-of-plane displacements generated are compared for all the three configurations. The effect of geometry and electrode layout are at first assessed in terms of purity of the shear horizontal mode; the most performing configuration is then further modified to enhance the amplitude and the signal to noise ratio of the generated mode. Design changes can then be predicted and suggested.

1. Introduction

In the field of ultrasonic testing, guided wave testing (UGWT) has witnessed a growing interest both in theoretical studies and industrial applications. The necessity of inspecting structures such as oil and gas pipelines or tanks in a reliable and fast way has often been met by this method of inspection (1). Guided waves are defined as mechanical waves travelling along the boundary of a structure (i.e. the thickness of the pipe) (2) where the reflection of the wave fronts between the two thickness boundaries enables the transmission of the generated signal up to 100 metres, with low attenuation when compared with bulk waves. In plates, guided wave modes are defined after Lamb, who proved theoretically the existence of these modes in a plate with traction-free boundary conditions (3). The symmetric and antisymmetric first Lamb modes are defined as S0 and A0 respectively, while the fundamental shear horizontal mode is defined as SH0.

The multimodal nature of guided waves and their dispersive behaviour requires careful tuning of the excitation in order to excite only one preferential mode. Alleyne and Cawley proposed a dry-coupled thickness-shear transducer for inspection of tubular structures (4): the removal of the liquid coupling enhanced the portability of the system and the generation of shear waves. However, the direct contact between the transducer and the waveguide required the application of a normal force applied on the top of the transducer to guarantee an adequate ultrasonic output through the generation of a shear stress imparting a shear displacement. The mechanical behaviour was then further studied by Engineer (5), who found a resonance force for the transducer at a frequency of 20 kHz: moreover, he proved experimentally that the amplitude of transmission of the transducer is enhanced until a threshold of 350 N, following a non-linear Hertzian contact law. The transducer proposed by Alleyne and Cawley was further modified by Elborn (6), who proposed a wrap-around electrode method to guarantee a robust electrical connection for the transducer.
In plate-like structures, the shear horizontal mode has experienced a continuous interest in exploitation due to its non-dispersive nature across the frequencies (7): Marquez studied arrays of thickness-shear transducers in order to generate a pure shear mode without any excitation of Lamb waves (8). Even though the mode purity of SH0 was enhanced, Marquez stated that a better result in term of mode purity could have been obtained by miniaturizing the transducer. The miniaturization of the transducer requires at first the understanding of the physical principles underlying its behaviour and which parameters influence the ultrasonic performance: Lowe et al (9) and Zennaro et al (10) have shown that both the geometry and the electrode layout of the transducer modify the ultrasonic performance. Boivin and Belanger also reported that the mass of a transducer for omnidirectional SH0 can cause the generation of an unwanted A0 mode (11).
Moghadam et al. developed a two dimensional analytical model to express the shear stress profile of a transducer and were able to tune the generation of Lamb modes by optimizing the shear stress profile with a genetic algorithm method (12); moreover, Gawronski et al. developed a semi-analytical model of a transducer and they studied different configurations of the transducer with genetic algorithm methods, with the objective of maximizing the amplitude of S0 or A0 (13).
The transducer in this paper (6) consists of an assembly (see section 2) with manufacturing constraints. The scope of this paper is to study some of the parameters of the transducer (geometry, materials, electrical connections) to understand how they affect the ultrasonic performance: in particular the increase in mode purity and amplitude of SH0.
The remainder of the paper is organized as follows: section 2 presents a brief description of the transducer, section 3 presents the computational model of the transducer and the results, and finally in section 4 some conclusions are outlined.

2. Piezoelectric transducer

2.1 Assembly

The piezoelectric transducer devised in (6) is made of three fundamental elements, a piezoelectric thickness-shear ceramic transducer, an alumina wear-plate and a backing block of steel.
Thickness shear piezoelectric elements are defined as devices where the application of an electric field orthogonal to the axis of polarization of the element causes a shear

deformation into the piezoelectric body (14); in this case the transducer is polarized along the length. The geometrical dimensions of the transducer are 13 x 3 x 0.5 mm.
The brittleness of the transducer and the necessity to apply a force to couple it to the waveguide require the use of an alumina wear-plate material where the geometrical dimensions correspond to the piezoelectric element. To increase the flexural stiffness of the transducer and to guarantee an appropriate distribution of the coupling force on the piezoelectric element, a cuboid mass of stainless steel of approximately 14 x 13 x 14 mm is used. The electrical connection to the piezoelectric element is obtained through a wrapped around electrode (6) and the cable configuration is not symmetrical to the centre of the cuboid.
Such an arrangement is represented in picture 1 as configuration A. Such a configuration with and without a wrapped around electrode was studied both numerically and experimentally (10). In this paper configuration A will be at first compared with a similar configuration where no hole but with a wrapped around electrode is present (configuration B); such a configuration will then be modified to remove the wrapped around electrode (configuration C). Configurations B and C also have the same backing mass geometry, which is different from the geometry of A. The three configurations are schematically presented in figure 2.

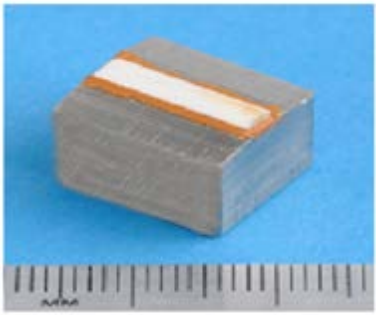

Figure 1. Configuration A of the transducer. Note the only the cuboid of steel (gray) and the alumina layer (white) can be seen.

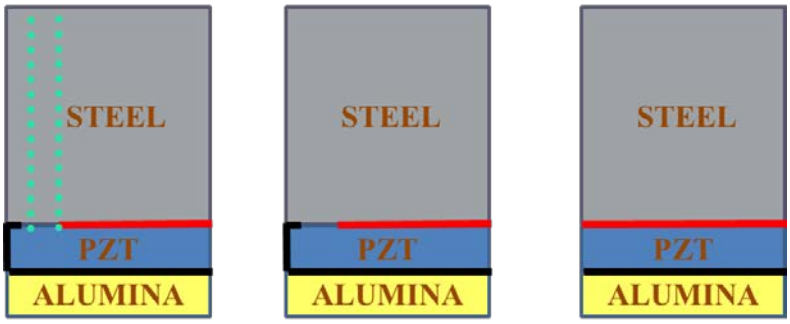

Figure 2. Configuration A, B and C respectively from left to right.

3. Frequency domain analysis

3.1 Numerical procedure for the frequency domain model

One of the fundamental requirements of the transducer is the capacity to excite a consistent guided wave response across the range of frequencies 20-100 kHz, i.e. a flat frequency response function without any resonance in the range of excitation. Thus, a frequency domain study was computed with the software Comsol Multiphysics in this range of excitation, with a discrete spacing between frequencies of 1 kHz, which have been shown to be capable of reproducing the behaviour of the transducer (11).
The electrostatics and solid physics interface of the solver were both used to adequately represent the behaviour of the transducer. A terminal voltage boundary condition was inserted on the top surface of the piezoelectric material; for configuration A and B the

ratio between the actuation length and the full length of the transducer was 0.77; for configuration C the ratio was 1, with an amplitude of 15 V (12).
As a waveguide, only a small plate of the radius of 15 mm was used: a low reflecting-boundary condition was inserted on every boundary of the plate, except on the boundary in contact with the waveguide. Thus any wave transmitted into the waveguide will propagate without being reflected, allowing the study of the interaction of the transducer with the interface.

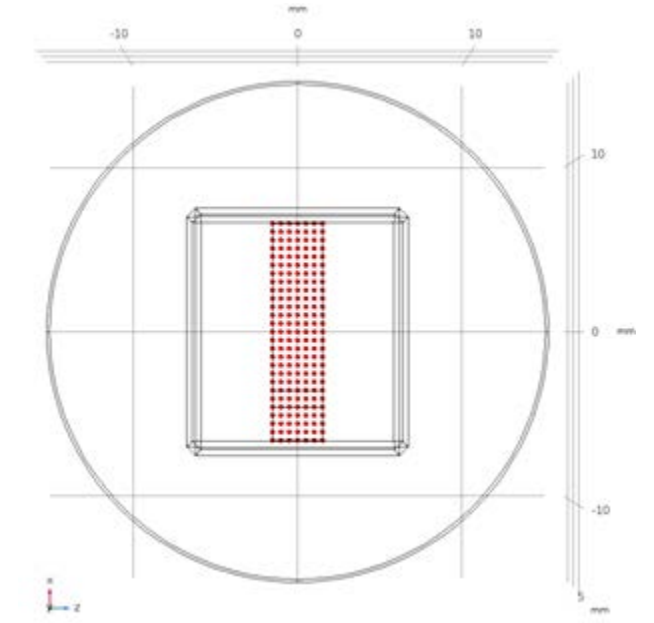

Figure 3. Top view of configuration B. Note the grid of points defined with red dots on the surface of the wear-plate.

3.2 Frequency response function

It is well known that the transmission of the signals is enabled by the friction of the wear-plate with the waveguide. Thus, it is of interest to calculate how the response changes at this interface. A grid of points was then defined on the lower surface of the wear-plate to extract information on the in-plane and out-of-plane displacement. The defined grid of points is represented in figure 3.

The frequency response function for configuration A is shown in figure 4. The peak in-plane displacement is plotted for five points chosen along the central line of the longitudinal axis. It is readily seen that a resonance is identified at 23 kHz: interestingly for this resonance the out-of-plane motion is higher than the in-plane. After this resonance the frequency response function is almost flat. The presence of a resonance at this frequency was already stated experimentally by Engineer (5), who also proved that this resonance is force dependent. It observed how, for the in-plane component, there is a difference in displacement for the points according to the position: as a matter of fact, the lower the displacement, the closer this point is to the wrap around electrode.
Therefore, to obtain a complete flat response along this range, parameters like stiffness of the backing mass and the geometry could be of interest to cancel this resonance and enable a full range of operation.
The same procedure was repeated to represent the frequency response function of configuration B. In this case it can be observed in figure 5 that both in-plane and out-of-plane motion experiences a diminution of displacement, probably attributable to the higher mass of the backing mass (no hole is now present). Moreover, the same design problem of a resonance at 23 kHz is still present. It is interesting to note how the in-plane displacement shows a similar pattern for configuration A and B.
Then the frequency response function is plotted for configuration C in figure 6. It can be noted that the in-plane displacement does not seem to change in comparison to B, while it appears that the out-of-plane motion seems to be diminished for configuration C, in the sense that the difference in the out-of-plane motion decreases among points.

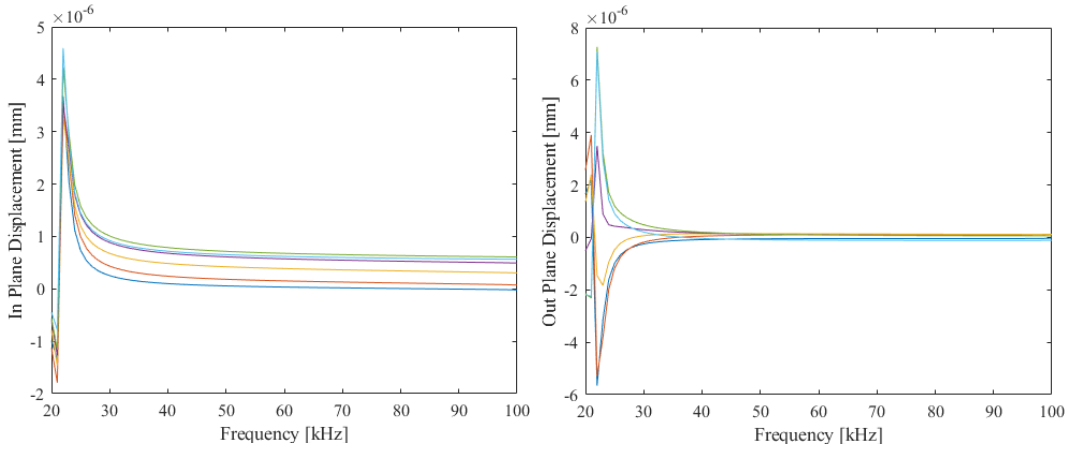

(b) **(b)**

Figure 4. Frequency response function for configuration A. In-plane (a) and Out-of-plane (b) are plotted.

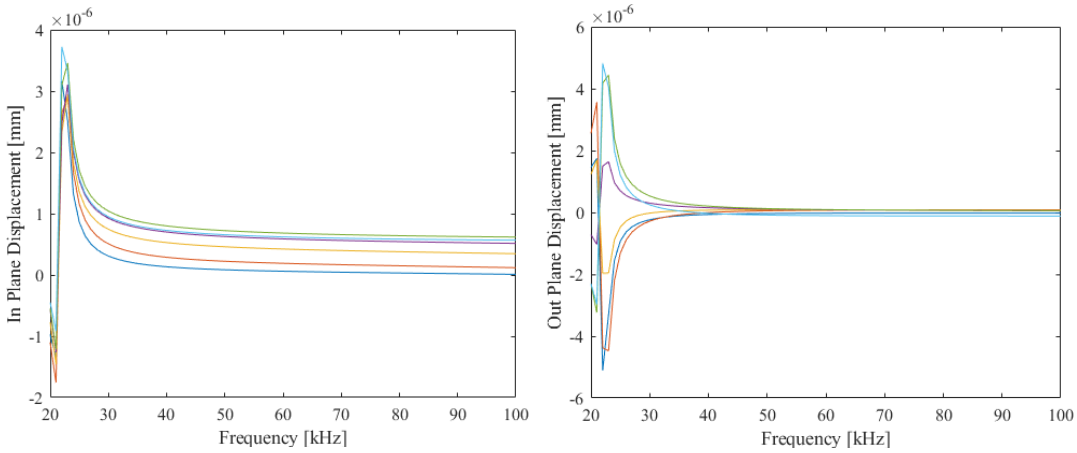

(a) **(b)**

Figure 5. Frequency response function for configuration B. In-plane (a) and Out-of-plane (b) are plotted.

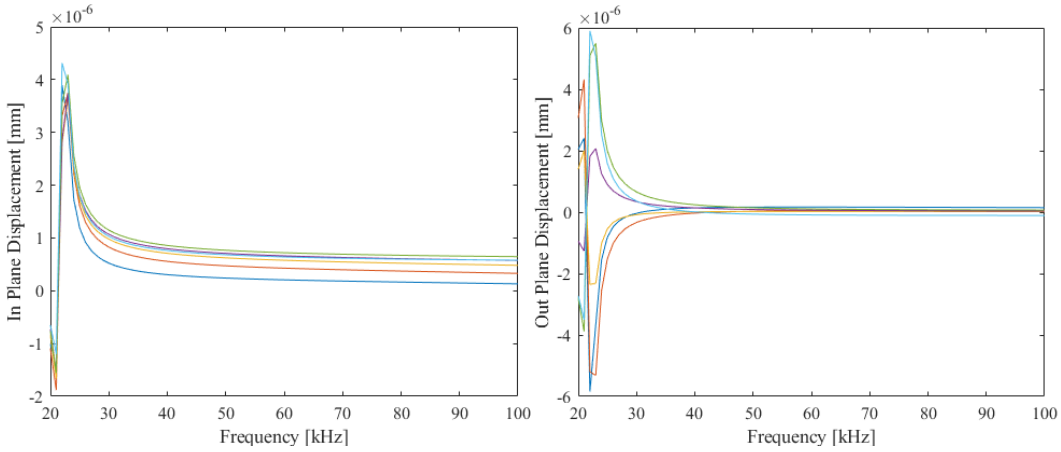

(a) **(b)**

Figure 6. Frequency response function for configuration B. In-plane (a) and Out-of-plane (b) are plotted.

3. Numerical analysis

3.1 Numerical procedure for the transient model

The transducer is modelled using the finite element method (9) using the commercial software Comsol Multiphysics with the physics interface “solid mechanics module”.
The transducer was placed at the centre of a steel plate of 0.3m radius and 3mm thickness: the radius of the plate was chosen as the minimum length to guarantee adequate separation between the S0 and A0 modes. In regards to the contact between the wear-plate and the waveguide, it was assumed that the two surfaces were perfectly flat, so that there is no relative movement.
The transducer was excited with a 5 cycle Hann windowed pulse with central frequency at 90 kHz: the excitation was represented numerically with a boundary load applied on the upper surface of the transducer in the time domain with an implicit solver, the alpha method. The mesh elements chosen for the study were of tetrahedral type: the mesh size was 3mm, according to the rule of 10 elements for wavelength, already validated in the literature (15). Dispersion curves were calculated with the software Disperse (16): for this particular geometrical configuration only S0, A0 and SHO should appear at the frequency of excitation of 90 kHz.
A picture of the imported FEA assembly and its mesh can be seen in figure 7, with the transducer inserted in the centre of the plate. The axes of vibration and expected direction on the wave modes are also represented. Along the longitudinal direction symmetric and antisymmetric modes are expected, while on the directional orthogonal to the axis of vibration the shear horizontal mode is expected.

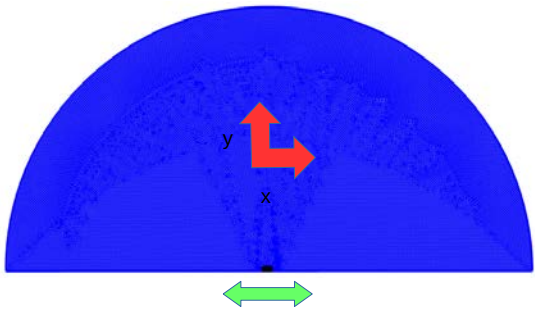

Figure 7. Picture of the mesh of the FEA model. The transducer is inserted in the centre: the green arrow represents the axis of vibration while x and y axis represent the longitudinal and transversal direction of motion respectively.

3.2 Numerical results for the transient model

The numerical surface plots for configurations A and B are shown in figure 8: the surface plot of in-plane displacement at 75μs shows that the shear horizontal mode is propagating along the transversal direction, while S0 and A0 are propagating on the longitudinal direction. At this particular time frame the symmetric Lamb mode at 75μs has already reached the border of the plate. The shear horizontal mode presents the highest amplitude, as the objective of research requires.
In figure 10, the results for the in plane displacement at a receiving point on the border of the plate are shown for a comparison between configuration A and B: results are normalized to the maximum of the in-plane displacement of configuration A, which in the frequency response function has shown the higher displacement. The equation for the time of arrival (15) indicates that the shear horizontal mode should arrive at 93.7μs, and such a result is confirmed numerically.

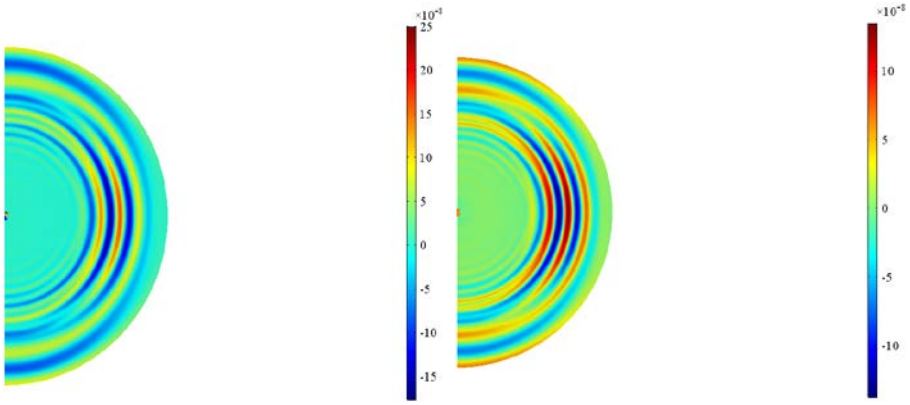

(a) **(b)**

Figure 9. In-plane surface displacement for configuration A (a) and B (b)

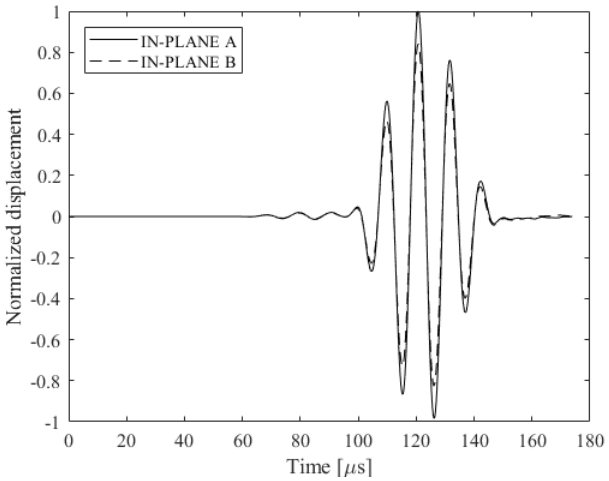

Figure 10. In-plane displacement at the receiving point orthogonal to the axis of vibration.

As shown in the frequency domain model, there is a reduction of almost 20% of the peak amplitude of the shear horizontal mode. Thus, configuration B would be detrimental in terms of the generation of the shear horizontal mode; following the results in frequency domain, the data for configuration C are not plotted, since the in-plane displacement is the same as for configuration B.

However, in the frequency domain case it was shown that the three configurations show some differences for the out-of-plane displacement: such a difference could be advantageous to assess the mode purity of the shear horizontal mode and control the wave modes generated along the orthogonal direction of excitation, since in Zennaro et al. (10) it was shown that a thickness-shear transducer can generate a A0 mode along the orthogonal direction of excitation.

Thus, the out-of-plane surface plot for the three configurations are plotted in figure 11 and figure 12.

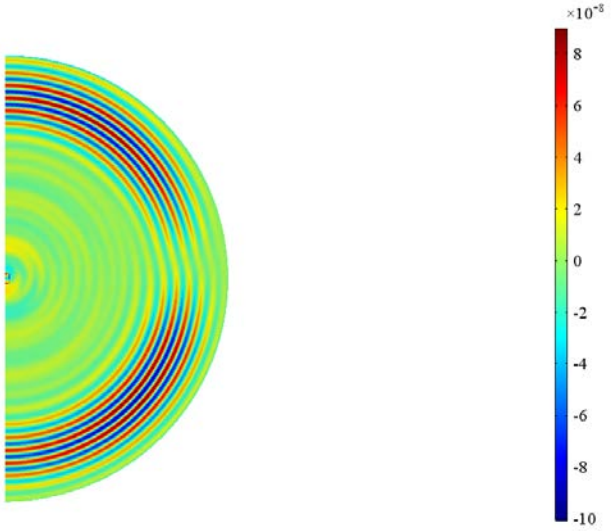

Figure 11.Numerical plot of out-plane surface displacement mode for configuration A.

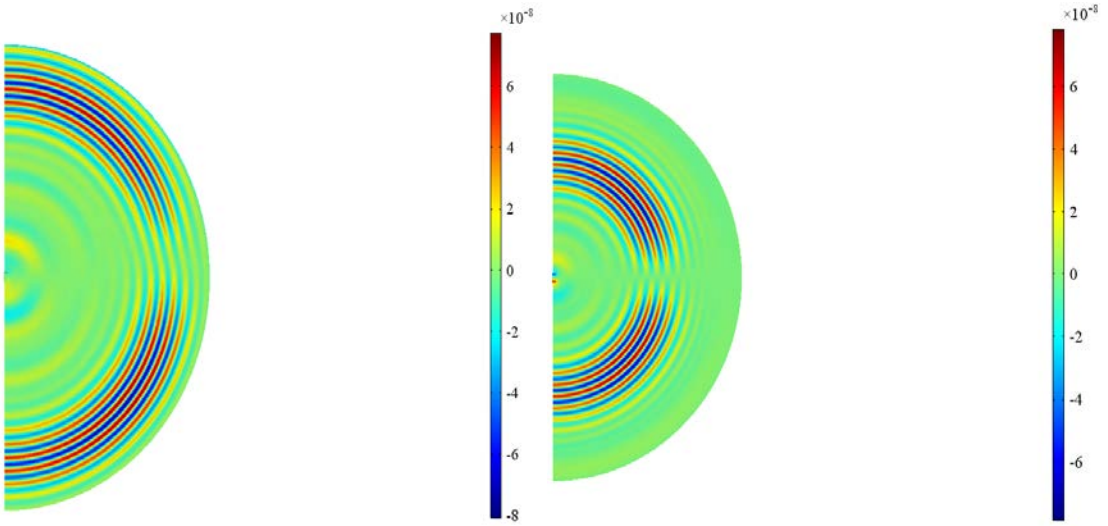

(a) **(b)**

Figure 12.Numerical plot of out-plane surface displacement mode for configuration B (a) and C (b).

In figure 12, configuration A and B show an out-of-plane displacement which is propagating almost all around the diameter of the circumference, with a slight asymmetry in the propagating wave: such an asymmetry could be recognised as due to the wrap-around electrode (approximately 20 degrees away from the axis). On the other hand, configuration C shows a symmetric distribution of the out-of-plane motion along the circumference. Moreover, along the axis orthogonal to the axis of vibration the out-of-plane displacement seems much a lower. Such an intuition is confirmed by the plot of the normalized out-of-plane displacement on the receiving point where only SH0 is expected: data are normalized to the maximum of the out-of-plane of configuration A, which presents the higher peak displacement.

As for the in-plane, in this case the out-of-plane displacement between configuration A and B is simply scaling down of 20 % as shown in figure 13: the third configuration

instead shows a remarkable decrease and the wave propagation of the A0 becomes almost negligible.

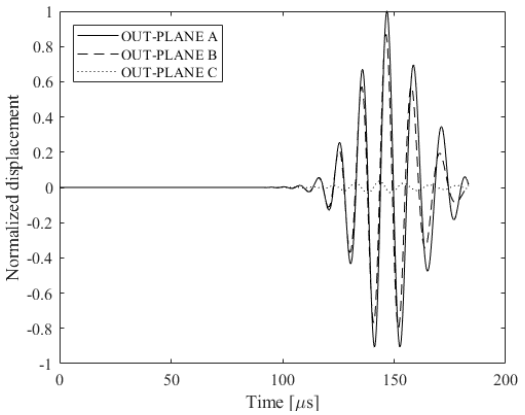

Figure 13. Plot of the out-of-plane displacement along the axis orthogonal to the axis of vibration.

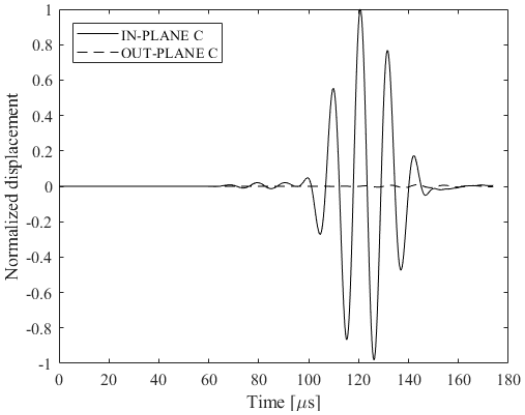

Figure 14. Plot of the in- and out-of-plane displacement along the axis orthogonal to the axis of vibration.

Then, the in- and out-of-plane displacement for configuration C is plotted in figure 14. The comparison between the two modes show that the difference of amplitude is almost of 95 %, thus the propagation of A0 along the orthogonal direction becomes negligible. Such a configuration would then to be chosen in order to guarantee a purer SH0 mode.

4. Conclusions

The frequency response function of different transducers configurations has been computed numerically. While the in-plane displacement seems to be influenced by the mass of the transducer, the position of the electrode seems to influence the out-of-plane displacement.

The results in the frequency domain analysis were then compared with the results obtained in the transient analysis with a much larger waveguide. The results in the time domain shows that configuration A leads to a higher SH0 mode, while configuration B shows a reduced displacement in terms of the shear horizontal mode in comparison to configuration A. However, both configuration A and B shows the presence of an unwanted A0 mode being generated along the direction of the shear horizontal mode. Configuration C gives a 95% reduction in the amplitude of the unwanted out of plane component when compared with configurations with a wrap around electrode.

It could be speculated that such a mode for configuration C would be buried in the noise level in a field-trial application, thus enabling almost the perfect generation of a shear horizontal mode.

However, more work is required to obtain a flat frequency response function in the range of excitation: the stiffness and the geometry of the backing mass could then be modified in order to cancel the resonance at 23 kHz.

The configuration C, which is found to be the best in terms of the generation of the SH0 mode, can now be studied to be further developed numerically and tested experimentally.

References and footnotes

The support of Loughborough University and Lloyd’s Registered Foundation for this publication is fully acknowledged.

References and footnotes

1. P J Mudge, ‘Field application of the Teletest long range ultrasonic testing technique’, Insight, Vol 43, No 2, pp 93-96, 2001.
2. J L Rose, ‘Ultrasonic guided waves in solid media’, Cambridge University Press, 2014.
3. H Lamb, ‘On waves in an elastic plate’, Proceedings of the Royal Society of London. Series A, vol. 93, no. 648, pp 114-128, 1916.
4. D N Alleyne and P. Cawley, “The excitation of Lamb waves in pipes using dry coupled piezoelectric transducer”, J. Nondestructive. Eval. , vol 15, no 1, pp 11-20, 1996.
5. B, Engineer, ‘The mechanical and resonant behaviour of a dry coupled thickness shear PZT transducer used for guided wave testing in pipeline’, Ph.D. dissertation, Dept. Mech. Aer. Civ. Eng., Brunel University, London, UK, 2013.
6. B J, Elborn. ‘Performance enhancements in an ultrasonic guided wave pipe inspection system’ Ph.D. dissertation, Dept. Mech. Aer. Civ.Eng, Brunel University, London, UK, 2015.
7. K F Graff, ‘Wave motion in elastic solids’, Courier Corporation, 2012.
8. Marques, ‘Omnidirectional and unidirectional SH0 mode transducer arrays for guided wave evaluation of plate-like structures’, Ph.D. dissertation, Dept. Mech. Aer. Civ. Eng., Brunel University, London, 2016.
9. P.S. Lowe, S. Fateri, R. Sanderson, N.V. Boulgouris ‘Finite element modelling of the interaction of ultrasonic guided waves with coupled piezoelectric transducers', Insight, vol 56 no 9, pp 1-5, 2014.
10. M Zennaro, D J O’Boy, P S Lowe ‘Performance enhancements of thickness-shear transducers for guided wave applications’, to be submitted
11. V M Chillara, B Ren, C L Lissenden. ‘Guided wave mode selection for inhomogeneous elastic waveguides using frequency domain finite element approach’, Ultrasonics, vol 67, pp 199-211, 2016.
12. M. Zennaro, A. Haig, O’Boy, D. J., S. J. Walsh, ‘Characterisation of the Vibration of an Ultrasonic Transducer for Guided Waves Applications’ Applied Physics, System Science and Computers II: Proceedings of the 2nd International Conference on Applied Physics, System Science and Computers (APSAC2017), September 27-29, 2017, Dubrovnik, Croatia. Vol. 489. Springer, 2018.
11. P. Belanger, G, Boivin, ‘Development of a low frequency omnidirectional piezoelectric shear horizontal wave transducer’, Smart Materials and Structures, vol 25, pp 045024, 2016.
12. P Y Moghadam, N Quaegebeur, P Masson, ‘Mode selective generation of guided waves by systematic optimization of the interfacial shear stress profile’ Smart Materials and Structures, vol 24, no. 1, 015003, 2014.
13. M, Gawronski, M, Miszczynski, P Kijanka, T Stepinski, T Uhl, J Lis, P Packo, ‘A semi-analytical approach to design of a transducer for selective wave generation’, Structural Health Monitoring, vol 16, no 5, pp 583-593, 2017.
14. N, Aurelle, D Roche, C Richard, P Gonnard, ‘Sample aspect ratio influence on the shear coefficients measurements of a piezoelectric bar’ In Applications of Ferroelectrics, ISAF'94., Proceedings of the Ninth IEEE International Symposium on, pp 162-165, 1994.
15. P S, Lowe, T Scholehwar, J Yau, J Kanfoud, T Gan, C Selcuk, ‘Flexible Shear Mode Transducer for Structural Health Monitoring using Ultrasonic Guided Waves’, IEEE Transactions on Industrial Informatics, 2017.
16. B Pavlakovic, M Lowe, D Alleyne, P Cawley, ‘Disperse: a general purpose program for creating dispersion curves’ In Review of progress in quantitative nondestructive evaluation, pp 185-192. Springer, Boston, MA, 1997.